



Asian Research Association



## Phase equilibria in the $\text{CeO}_2\text{--La}_2\text{O}_3\text{--Gd}_2\text{O}_3$ system at 1250 and 1500 °C

O.A. Kornienko <sup>a,\*</sup>, O.I. Bykov <sup>a</sup>, A.V. Sameljuk <sup>a</sup>, Yu.M. Bataiev <sup>a</sup>, S.V. Yushkevych <sup>a</sup>

<sup>a</sup> Frantsevich Institute for Materials Science Problems NAS, Kiev – UKRAINE, 3 Krzhizhanovsky str., Kyiv, 03680, Ukraine.

\* Corresponding author email: [kornienkooksana@ukr.net](mailto:kornienkooksana@ukr.net)

DOI: <https://doi.org/10.34256/irjmt2143>

Received: 19-05-2021, Revised: 06-06-2021, Accepted: 08-06-2021, Published: 10-06-2021

**Abstract:** Materials based on cerium oxide, stabilized by oxides of rare earth elements, are promising for use in medicine, energy and mechanical engineering due to the uniqueness of their properties. State diagrams of  $\text{CeO}_2\text{--La}_2\text{O}_3\text{--Ln}_2\text{O}_3$  systems are the physicochemical basis for the creation of solid electrolytes for fuel cells, oxygen gas sensors, catalyst carriers, protective coatings on alloys, etc. Phase equilibria and structural transformations in  $\text{CeO}_2\text{--La}_2\text{O}_3\text{--Gd}_2\text{O}_3$  systems at temperatures 1250 and 1500 °C and in the binary system  $\text{La}_2\text{O}_3\text{--Gd}_2\text{O}_3$  at temperatures 1100, 1500 and 1600 °C in the whole range of concentrations were investigated using X-ray phase and microstructural analyzes. It was found that solid solutions based on cubic (F) modification with  $\text{CeO}_2$  fluorite type, monoclinic (B) and cubic (C) modifications of  $\text{Gd}_2\text{O}_3$  and hexagonal (A) modification of  $\text{La}_2\text{O}_3$  are formed in the ternary system  $\text{CeO}_2\text{--La}_2\text{O}_3\text{--Gd}_2\text{O}_3$ . The boundaries of the phase fields and the periods of the crystal lattices of the formed phases are determined. It is established that in the  $\text{CeO}_2\text{--La}_2\text{O}_3\text{--Gd}_2\text{O}_3$  system at 1250 and 1500 °C the phases of cubic symmetry are in equilibrium: on the basis of F– $\text{CeO}_2$  with the spatial group  $Fm\bar{3}m$  and C-phase on the basis of  $\text{Gd}_2\text{O}_3$  with the spatial group  $Ia\bar{3}$ . As the temperature decreases, there is a narrowing of all areas of homogeneity.

**Keywords:** Lanthanum and gadolinia, Cerium oxides, Phase equilibrium, Solid solutions, Functional and structural ceramics.

### 1. Introduction

Materials based on cerium oxides and lanthanides are widely used in high-tech industries. In recent years, cerium dioxide has been used as a protective coating that absorbs UV radiation, as the main component of polishing mixtures and abrasives, in sensor devices that allow to determine the minimum amount of impurities in gas mixtures, solid electrolytes for fuel cells and others. [1-4]. Highly dispersed cerium dioxide and solid solutions based on it are part of three-way catalysts designed for efficient combustion of car exhaust gases, used in selective oxidation reactions in the dehydrogenation of alcohols, etc. [4].

Physico-chemical design of new materials can not be performed without basic fundamental information about the original components and their interaction under different conditions. The state diagram of the  $\text{CeO}_2\text{--La}_2\text{O}_3\text{--Gd}_2\text{O}_3$  system is a physicochemical basis for the creation of materials for structural and functional purposes. There are no data on the thermodynamic stability of solid solutions based on oxides of cerium, lanthanum and gadolinium in the literature, which

necessitates the study of phase equilibria in the ternary system  $\text{CeO}_2\text{--La}_2\text{O}_3\text{--Gd}_2\text{O}_3$ .

The binary system  $\text{CeO}_2\text{--La}_2\text{O}_3$  was studied in [5–13]. In our opinion, the most reliable data on phase equilibria in this system are presented in [13]. It is established that two types of solid solutions are formed in the  $\text{CeO}_2\text{--La}_2\text{O}_3$  system: cubic phase F based on  $\text{CeO}_2$  fluorite and hexagonal phase A based on the compound  $\text{La}_2\text{O}_3$ , the homogeneity regions of which are separated by a two-phase field (A + F). The limiting solubility of  $\text{La}_2\text{O}_3$  in the crystal lattice of  $\text{CeO}_2$  is 49% (mol) in the temperature range 1500–1100 °C [13]. The solubility of  $\text{CeO}_2$  in the hexagonal modification of A- $\text{La}_2\text{O}_3$  is 25 mol % at 1500 °C and 15 mol % at 1100 °C [13].

The  $\text{CeO}_2\text{--Gd}_2\text{O}_3$  system has a structure similar to the above-mentioned system [14–21]. At the same time, these systems have some differences related to the  $\text{La}_2\text{O}_3$  and  $\text{Gd}_2\text{O}_3$  polymorphisms. In the  $\text{CeO}_2\text{--Gd}_2\text{O}_3$  system in the temperature range 1500–600 °C, solid solutions with cubic phase F of fluorite type ( $\text{CeO}_2$ ) and cubic C based on structural type  $\text{Tl}_2\text{O}_3$  ( $\text{Gd}_2\text{O}_3$ ) are formed, as well as solid solutions based on monoclinic modification of rare

earth elements (B-Gd<sub>2</sub>O<sub>3</sub>) [14, 16, 19]. The boundaries of the regions of homogeneity of solid solutions based on F-CeO<sub>2</sub>, C- and B-Sm<sub>2</sub>O<sub>3</sub> correspond to the compositions of 10–15, 65–70 and 80–85, 98–99 mol % Gd<sub>2</sub>O<sub>3</sub> at 1500 °C [14] and 10–15, 85–80 mol % Gd<sub>2</sub>O<sub>3</sub> at 1100 °C [16], as well as 5–10, 90–95 mol % Gd<sub>2</sub>O<sub>3</sub> at 600 °C [19]. It is established that at a reduced temperature from 1500 to 1100 °C the number of phase fields decreases due to the fact that the monoclinic B - modification of Gd<sub>2</sub>O<sub>3</sub> exists above 1250 °C [22].

The phase relations and structure of the phases formed in the La<sub>2</sub>O<sub>3</sub>–Gd<sub>2</sub>O<sub>3</sub> system were studied in [22–31]. Graphic interpretation of the obtained data is shown in Figure 1.

It is established that in the La<sub>2</sub>O<sub>3</sub>–Gd<sub>2</sub>O<sub>3</sub> system three types of continuous solid solutions are formed on the basis of hexagonal (A and H) and cubic (X) modifications of REE oxides. A limited region of homogeneity was found on the basis of monoclinic (B) modification of Gd<sub>2</sub>O<sub>3</sub>. The maximum temperature of the existence of a solid solution based on B-Gd<sub>2</sub>O<sub>3</sub> is 2080 °C, which corresponds to the phase transformation temperature B ⇌ A of pure Gd<sub>2</sub>O<sub>3</sub>. The solubility of La<sub>2</sub>O<sub>3</sub> in B-Gd<sub>2</sub>O<sub>3</sub> is: 10 mol % at 2020 °C, 20 mol % at 1900 °C and 50 mol % at 1580 °C [22].

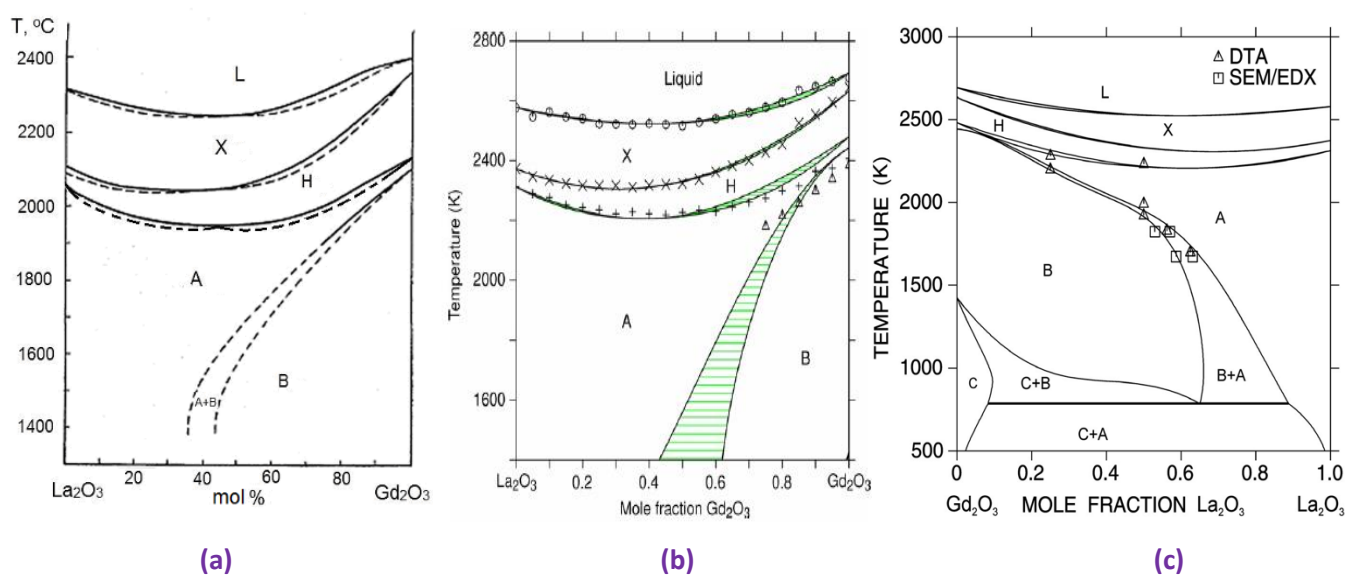


Figure 1. Phase diagram of the La<sub>2</sub>O<sub>3</sub>–Gd<sub>2</sub>O<sub>3</sub> system: (a) – [22], (b) – [23], (c) – [29].

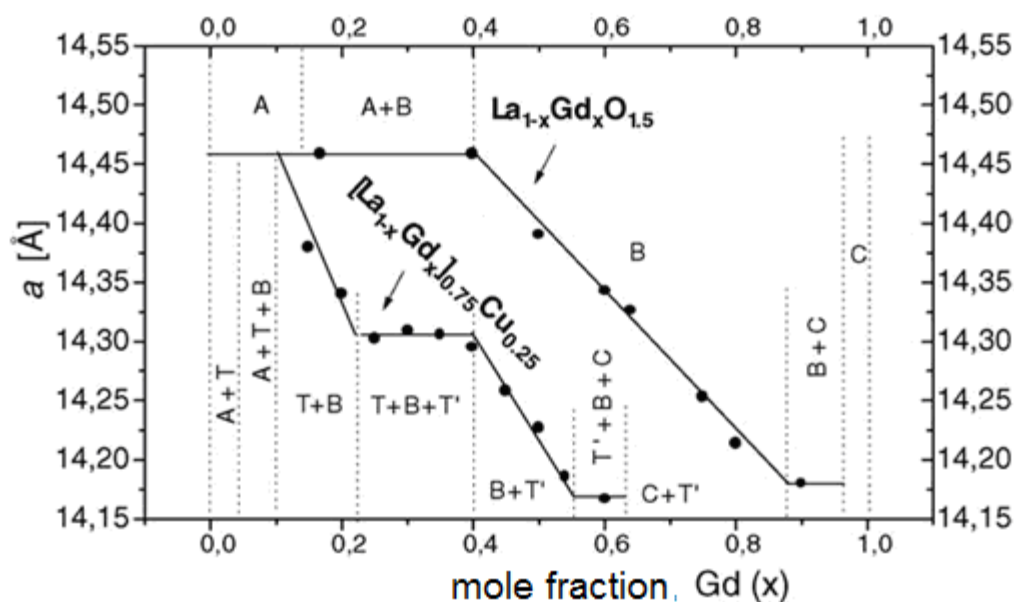


Figure 2. Phase boundaries of the (B) phase, determined via its c-lattice parameter variation, the latter calculated based on X-ray diffraction of 0.25 at. % Cu series and of Cu-free La<sub>(1-x)</sub>Gd<sub>x</sub>O<sub>1.5</sub> type one [26]

The phase transition  $A \rightleftharpoons H$  in the  $\text{La}_2\text{O}_3\text{--Gd}_2\text{O}_3$  system was recorded only by thermal analysis in the presence of an exothermic effect on the cooling curves. The system is characterized by a minimum near the composition of 60 mol %  $\text{La}_2\text{O}_3$  and  $\sim 2300$  °C [22].

At a temperature of 950 °C in the system  $\text{La}_2\text{O}_3\text{--Gd}_2\text{O}_3$  wide regions of homogeneity are formed on the basis of hexagonal modification of lanthanum oxide and monoclinic (B) modification of  $\text{Gd}_2\text{O}_3$ , as well as a small region of homogeneity of C- $\text{Gd}_2\text{O}_3$ . The dependence of the parameters of the unit cells of solid solutions formed in the  $\text{La}_2\text{O}_3\text{--Gd}_2\text{O}_3$  system on the concentration of gadolinium oxide at 950 °C is presented in Figure 2 [26].

Thus, the phase equilibria in the  $\text{La}_2\text{O}_3\text{--Gd}_2\text{O}_3$  system are most reliably represented from the melting temperatures up to  $\sim 2000$  °C. While information on phase equilibria at lower temperatures is not consistent with each other and requires further research.

## 2. Experiment

Cerium nitrate salt  $\text{Ce}(\text{NO}_3)_3 \cdot 6\text{H}_2\text{O}$ , as well as oxides  $\text{La}_2\text{O}_3$  (brand *LaO-1*) and  $\text{Gd}_2\text{O}_3$  (brand *GdO-D*) with the content of the main component of 99.99% were used as starting materials. Preliminary starting oxides were dried in a laboratory muffle furnace (*SNOL 7,2/1100 LSC21*) at 600 °C (2 h). A concentration step of 1 to 5 mol% was used to prepare the charge. Samples of oxides were dissolved in  $\text{HNO}_3$  (1:1), evaporated and calcined at 800 °C for 2 hours. The synthesized powders were compressed into tablets  $\varnothing = 5$  mm,  $h = 4 - 5$  mm under a pressure of 10–30 MPa. The obtained samples for the study of phase equilibria in the ternary system  $\text{CeO}_2\text{--La}_2\text{O}_3\text{--Gd}_2\text{O}_3$  at 1500 °C were subjected to a two-stage heat treatment: calcination in a laboratory muffle furnace (*SNOL 10/1300 LHM01*) with heaters H23U5T (fehral) at 1250 °C during 6200 h., which allowing get rid of nitrate residues, and annealing in a high-temperature furnace (*Micropyretics Heaters International M18-40*) with molybdenum disilicide heaters ( $\text{MoSi}_2$ ) at 1500 °C for 130 h. in air, resulting in diffusion-controlled leveling of the composition in accordance with the state diagram of the system. For homogenization of charges in the double system  $\text{La}_2\text{O}_3\text{--Gd}_2\text{O}_3$  the multistage mode of heat treatment is chosen:  $T_1 = 1100$  °C for 10000 h.,  $T_2 = 1500$  °C for 225 h. and  $T_3 = 1600$  °C for 10 h. The samples were heated from room temperature to the desired temperature at a rate of 3.5 deg./min. The heat treatment of the samples was continuous. Cooling was performed together with the oven.

Preparation of samples for microstructural studies was performed on a Buehler grinding and polishing machine. Microstructures were studied on a scanning electron microscope SUPERPROBE-733 (*JEOL, Japan, Palo Alto, CA*) in back-reflected electrons (BSE) on undigested sections of annealed samples with a gold-plated sample.

On the DRON-3 diffractometer (*Joint Stock Company "Bourestnik"*), at room temperature ( $\text{CuK}\alpha$ -radiation, Ni-filter) X-ray phase analysis (XRF) of the samples was performed. The modes used in the study were as follows - scanning step was 0.05-0.1 deg, exposure 4 s in the range of angles  $2\theta$  from 10 to 100°. The result of the experiment is the dependence of the intensity of diffracted radiation on the angle of reflection. The International Powder Standards Committee database (JSPDS International Center for Diffraction Data 1999) was used to identify the obtained X-ray diffraction results.

## 3. Results and Discussion

### 3.1 Diagram of the state of the $\text{La}_2\text{O}_3\text{--Gd}_2\text{O}_3$ system

Studies of the solid-phase interaction of  $\text{La}_2\text{O}_3$  (hexagonal modification, A) and  $\text{Gd}_2\text{O}_3$  (monoclinic B-modification of lanthanide oxides) at 1600, 1500 °C showed that two types of solid solutions are formed in the  $\text{La}_2\text{O}_3\text{--Gd}_2\text{O}_3$  system: based on hexagonal A- $\text{La}_2\text{O}_3$  modification and monoclinic modification of B- $\text{Gd}_2\text{O}_3$ , which are separated by a two-phase field (A + B). As the temperature decreases, the number of phase fields increases due to polymorphic transformations of  $\text{Gd}_2\text{O}_3$  and the formation of cubic solid solutions of C- $\text{Gd}_2\text{O}_3$ , (Figure 3).

The initial chemical and phase compositions of the samples after heat treatment at 1600, 1500 and 1100 °C, the parameters of the elementary cells of the phases that are in equilibrium at the specified temperatures are given in supplementary tables 1–3, respectively.

The change in the crystal lattice period of the solid solution A- $\text{La}(\text{OH})_3$  depending on the concentration of  $\text{Gd}_2\text{O}_3$  at 1600, 1500 and 1100 °C is presented in Figure. 4. It was found that the solubility of  $\text{Gd}_2\text{O}_3$  in the hexagonal A-modification of  $\text{La}_2\text{O}_3$  is 16 mol % at 1100 °C, 31 mol % at 1500 °C and 39 mol % at 1600 °C. The parameters of the unit cell vary from  $a = 0.6523$  nm,  $c = 0.3855$  nm for pure  $\text{La}(\text{OH})_3$  to  $a = 0.6494$  nm,  $c = 0.3797$  nm for a two-phase sample (A + B) of 80 mol %  $\text{La}_2\text{O}_3\text{--}20$  mol %  $\text{Gd}_2\text{O}_3$  (1100 °C) and up to  $a = 0.6461$  nm,  $c = 0.3747$  nm for a two-phase sample (A + B) of 65 mol %  $\text{La}_2\text{O}_3\text{--}35$  mol %  $\text{Gd}_2\text{O}_3$  (1500 °C), as well as up to  $a =$

0.6447 nm,  $c = 0.3716$  nm for a two-phase sample (A + B) of 60 mol %  $\text{La}_2\text{O}_3$ –40 mol %  $\text{Gd}_2\text{O}_3$  (1600 °C). According to X-ray diffraction, in samples containing from 100 to 35 mol %  $\text{La}_2\text{O}_3$ , instead of the hexagonal phase A- $\text{La}_2\text{O}_3$ , a hexagonal modification of lanthanum hydroxide A- $\text{La}(\text{OH})_3$  is formed, as lanthanum oxide hydrates in air (Figure 5).

The solubility of  $\text{La}_2\text{O}_3$  in monoclinic B-modification is 31, 40 and 62 mol % at 1600 1500 and 1100 °C, respectively. The unit cell parameters vary from  $a = 1.4335$  nm,  $c = 0.3566$  nm,  $b = 0.8813$  nm,  $\beta = 91.85$

for pure  $\text{Gd}_2\text{O}_3$  to  $a = 1.4573$  nm,  $c = 0.3597$  nm,  $b = 0.8952$  nm,  $\beta = 92.40$  for the two-phase sample (A + B) composition of 35 mol %  $\text{La}_2\text{O}_3$  (1600 °C) and up to  $a = 1.4464$  nm,  $c = 0.3656$  nm,  $b = 0.8752$  nm,  $\beta = 91.44$  for a two-phase sample (A + B), containing 40 mol %  $\text{La}_2\text{O}_3$  (1500 °C) and from  $a = 1.6675$  nm,  $b = 0.6784$  nm,  $c = 0.8644$  nm,  $\beta = 1291.37$  for a two-phase composition (A + B), containing 65 mol %  $\text{La}_2\text{O}_3$  to  $a = 1.3940$  nm,  $b = 0.3606$  nm,  $c = 0.8844$  nm,  $\beta = 871.45$  for a two-phase sample (C + B), containing 20 mol %  $\text{La}_2\text{O}_3$  (1100 °C).

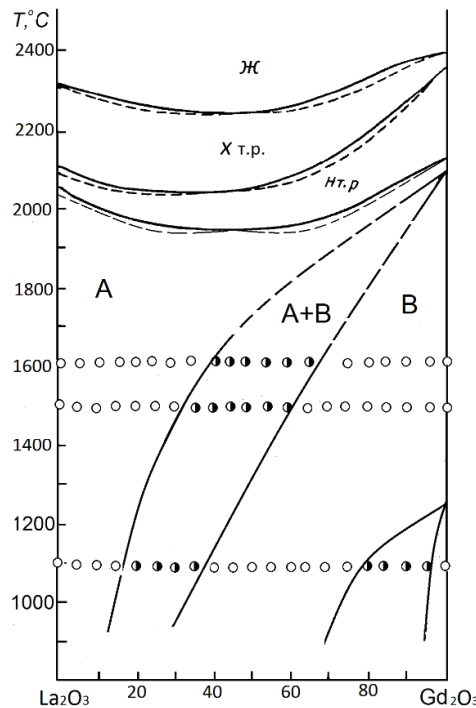


Figure 3. Phase diagram of the  $\text{La}_2\text{O}_3$ – $\text{Gd}_2\text{O}_3$  system: above 1500 °C according to [22] (○ - single-phase, ● - two-phase according to this study)

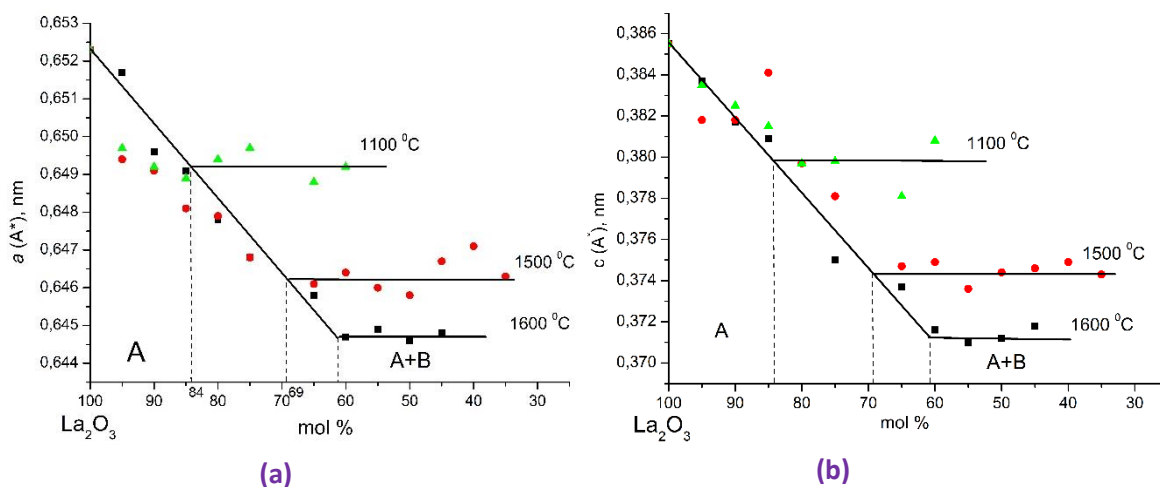
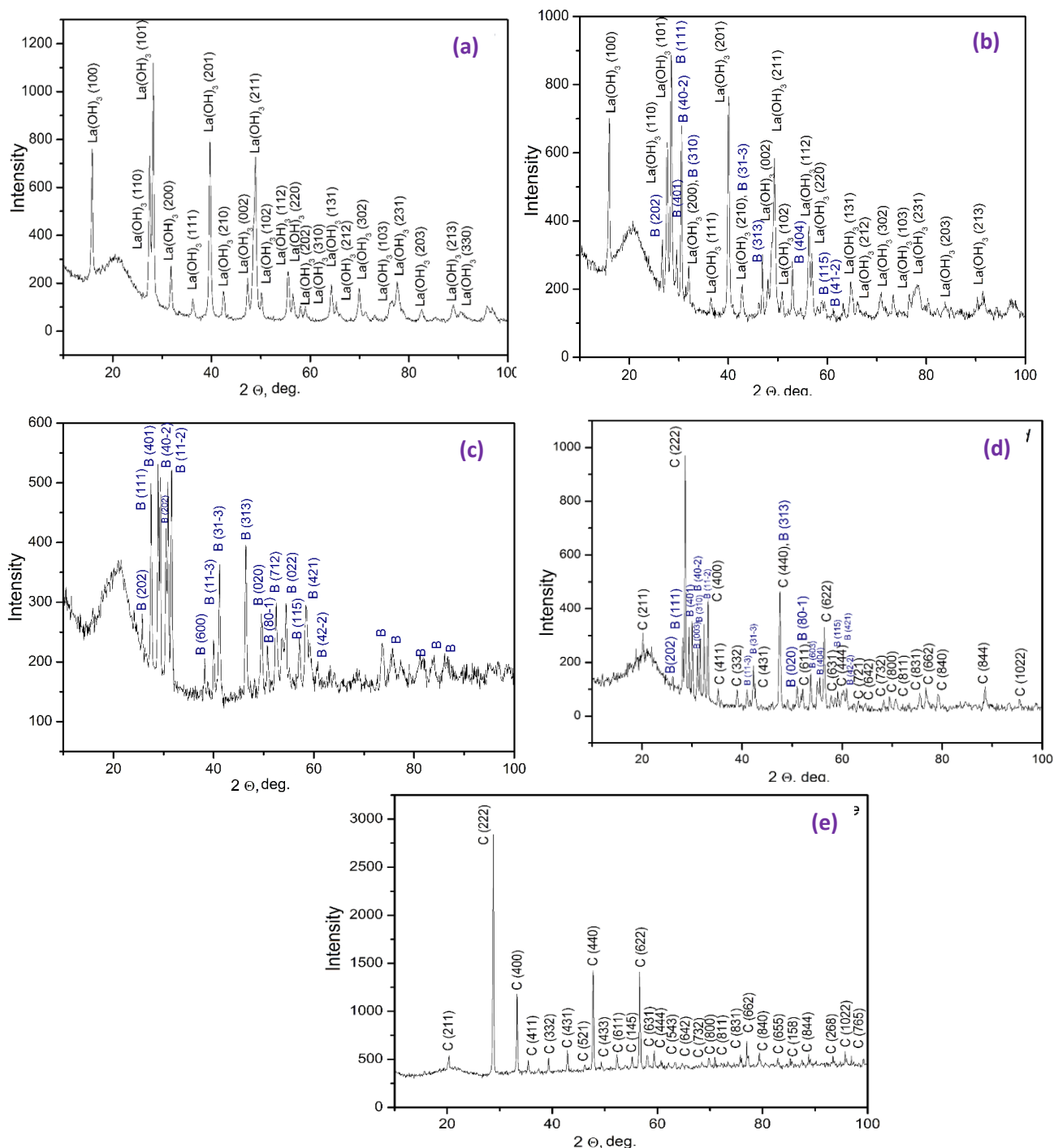


Figure 4. (a-b) Concentration dependences of the parameters of elementary cells of solid solutions based on A\* -  $\text{La}_2\text{O}_3$  in the system  $\text{La}_2\text{O}_3$ – $\text{Gd}_2\text{O}_3$  after heat treatment of samples at 1100, 1500, 1600°C



**Figure 5.** Diffractograms of samples of  $\text{La}_2\text{O}_3\text{--Gd}_2\text{O}_3$  system after heat treatment at  $1100^\circ\text{C}$ : **(a)** –100 mol %  $\text{La}_2\text{O}_3\text{--}0$  mol %  $\text{Gd}_2\text{O}_3$ , (A \* - $\text{La}(\text{OH})_3$ ); **(b)** - 75 mol %  $\text{La}_2\text{O}_3\text{--}25$  mol %  $\text{Gd}_2\text{O}_3$ , (A \* - $\text{La}(\text{OH})_3$ +<B>); **(c)** - 55 mol %  $\text{La}_2\text{O}_3\text{--}45$  mol %  $\text{Gd}_2\text{O}_3$ , (<B>); **(d)** - 5 mol %  $\text{La}_2\text{O}_3\text{--}95$  mol %  $\text{Gd}_2\text{O}_3$ , (<B>+<C>); **(e)** - 0 mol %  $\text{La}_2\text{O}_3\text{--}100$  mol %  $\text{Gd}_2\text{O}_3$ , (<C>).

It is established that the number of phase fields in the system increases with decreasing temperature. Due to the polymorphism of gadolinium oxide, a small region of homogeneity is formed on the basis of cubic solid solutions of C- $\text{Gd}_2\text{O}_3$ . The parameters of the unit cell C- $\text{Gd}_2\text{O}_3$  vary from  $a = 1.0777$  nm for pure  $\text{Gd}_2\text{O}_3$  to  $a =$

1.0816 nm for a two-phase sample (C + B), containing 5 mol %  $\text{La}_2\text{O}_3$ .

Diffractograms of samples characterizing the phase regions in the  $\text{La}_2\text{O}_3\text{--Gd}_2\text{O}_3$  system at  $1100^\circ\text{C}$  are presented in Figure. 5.

The microstructures of the samples after heat treatment at 1500 °C in the  $\text{La}_2\text{O}_3\text{--Gd}_2\text{O}_3$  system are presented in Figure 6. The microstructure of monoclinic B-modification of  $\text{Gd}_2\text{O}_3$  and solid solutions based on it are manifested in the form of differently oriented lamellar crystals. The microstructures of the samples characterizing the two-phase region (A + B) are presented in Figure 6, a-b. It follows from the presented microstructures that solid solutions based on hexagonal A-modification are characterized by the formation of cracks, this is probably due to the fact that  $\text{La}_2\text{O}_3$  in the air hydrates and turns into  $\text{La}(\text{OH})_3$ . This transition is marked by complete or partial destruction of the samples, as the volume of the unit cell increases from 0.128  $\text{nm}^2$  to 0.122  $\text{nm}^2$  for  $\text{La}_2\text{O}_3$  and  $\text{La}(\text{OH})_3$ , respectively. The other phase is represented by small inclusions of B- $\text{Gd}_2\text{O}_3$ , which are evenly distributed in the sample.

Thus, using the data [22] and the obtained results, a complete state diagram of the  $\text{La}_2\text{O}_3\text{--Gd}_2\text{O}_3$  system in the interval 800–2400 °C was constructed. This system is characterized by the formation of limited solid

solutions based on various crystalline modifications of the original components. It is established that the number of phase fields increases due to the decrease of temperature due to polymorphic transformations of  $\text{Gd}_2\text{O}_3$ . As mentioned earlier, this system was studied using thermodynamic calculations [23-24]. The results obtained in our study are slightly different from the data [23-24]. It is established that with decreasing temperature there is an expansion of the heterogeneous region (A + B). At the same time, the results obtained by us indicate a narrowing of this heterogeneous region with decreasing temperature. This narrowing is due to the complexity of the structure of this state diagram due to the formation of a region of homogeneity based on C- $\text{Gd}_2\text{O}_3$ . It also follows from the data obtained by us that the region of homogeneity based on A- $\text{La}_2\text{O}_3$  is characterized by a much narrower field of existence at all investigated temperatures in comparison with the data [23-24]. The results presented in this work are confirmed by the data of X-ray phase and microstructural analyzes, which are consistent with each other. The formation of new phases in the  $\text{La}_2\text{O}_3\text{--Gd}_2\text{O}_3$  system has not been established.

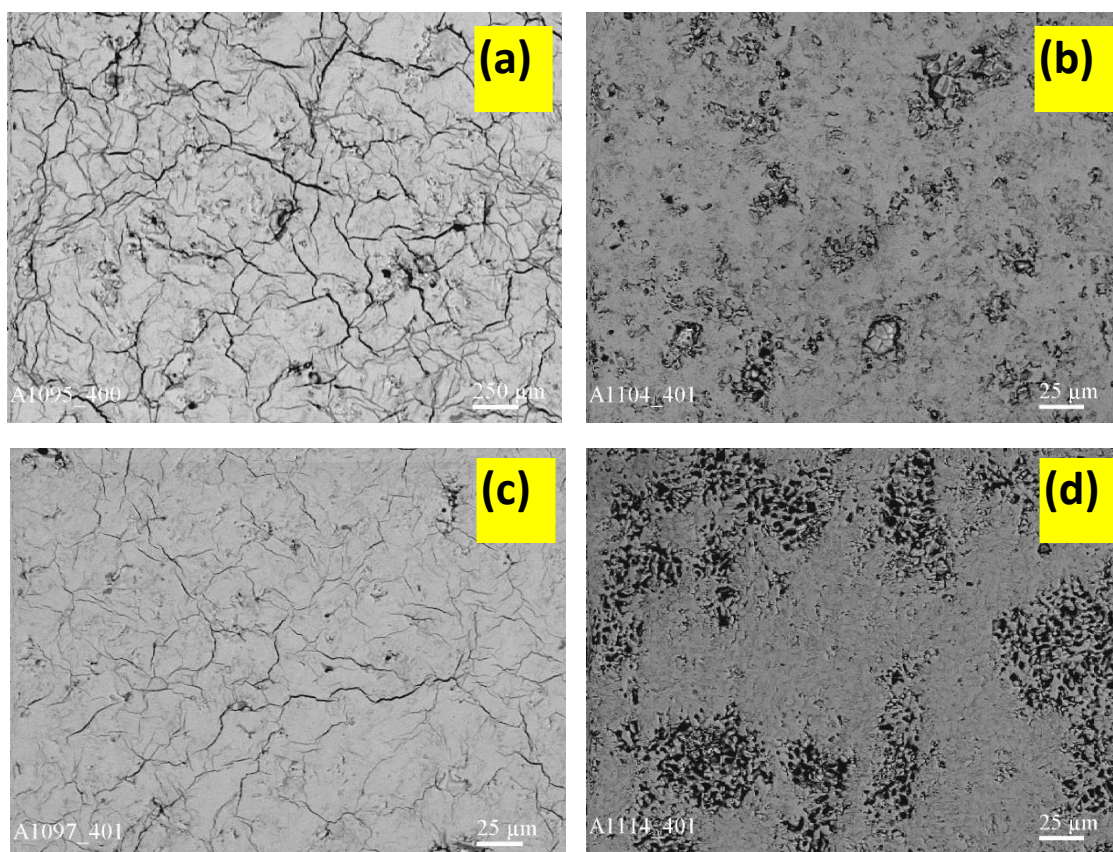


**Figure 6.** Microstructures of samples of the  $\text{La}_2\text{O}_3\text{--Gd}_2\text{O}_3$  system after heat treatment at 1500 °C: **(a)** - 45 mol %  $\text{La}_2\text{O}_3\text{--}55$  mol %  $\text{Gd}_2\text{O}_3$ , BSE $\times$ 400, B+A; **(b)** - 40 mol %  $\text{La}_2\text{O}_3\text{--}60$  mol %  $\text{Gd}_2\text{O}_3$ , BSE $\times$ 400, B+A; **(c)** - 25 mol %  $\text{La}_2\text{O}_3\text{--}75$  mol %  $\text{Gd}_2\text{O}_3$ , BSE $\times$ 400, B- $\text{Gd}_2\text{O}_3$ ; **(d)** - 0 mol %  $\text{La}_2\text{O}_3\text{--}100$  mol %  $\text{Gd}_2\text{O}_3$ , BSE $\times$ 400, B- $\text{Gd}_2\text{O}_3$ ;

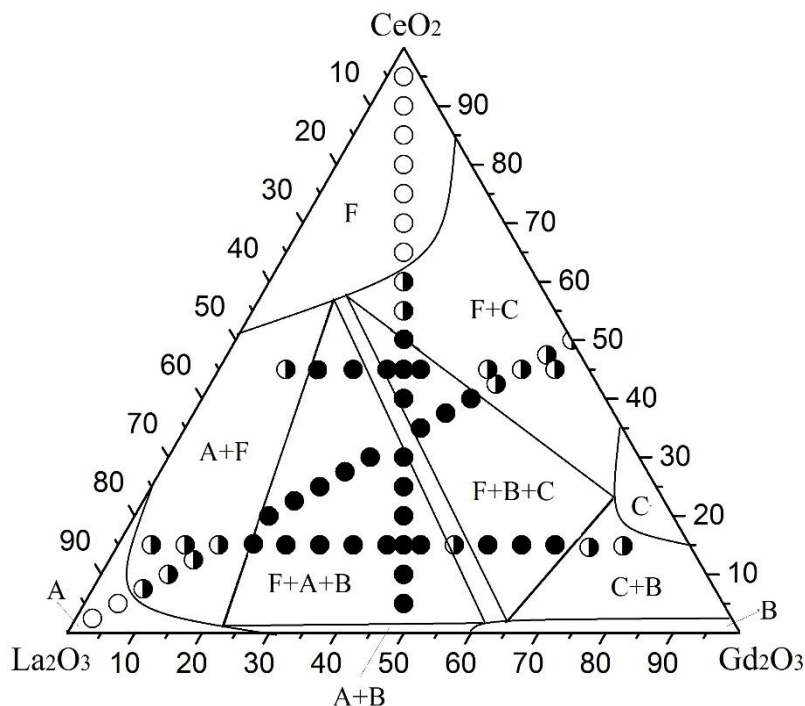


**Figure 7.** Isothermal cross section of the state diagram of the  $\text{CeO}_2\text{-La}_2\text{O}_3\text{-Gd}_2\text{O}_3$  system at 1500 °C (●- three-phase ◐ - two-phase and ○ - single-phase samples)

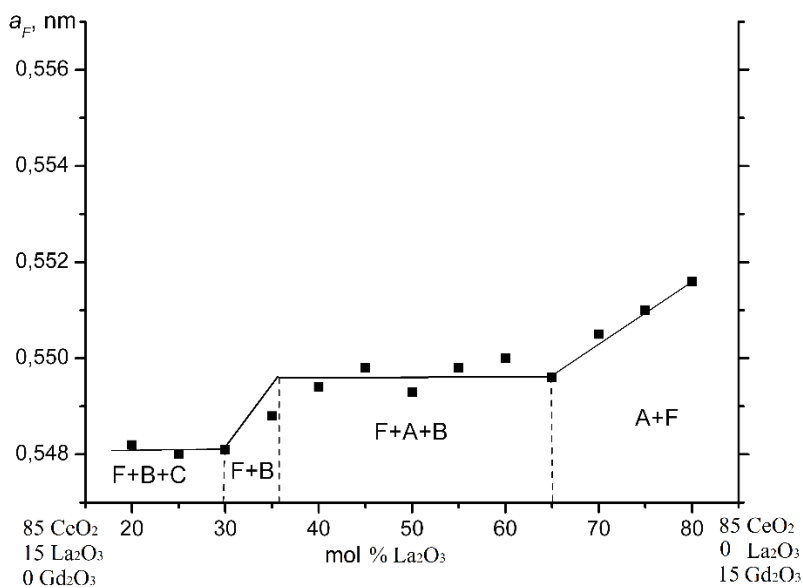


**Figure 8.** Concentration dependence of parameters of  $a$  elementary cells of solid solutions with fluorite-type structure (F- $\text{CeO}_2$ ) of  $\text{CeO}_2\text{-La}_2\text{O}_3\text{-Gd}_2\text{O}_3$  system along isoconcentrate of 15 mol %  $\text{CeO}_2$  after heat treatment of samples at 1500 °C

### 3.2 Isothermal cross section of the state diagram of the $\text{CeO}_2\text{-La}_2\text{O}_3\text{-Gd}_2\text{O}_3$ system at 1500 °C

To study the phase equilibria in the ternary system, samples were prepared whose compositions lie on two rays:  $\text{La}_2\text{O}_3\text{-(50 mol % CeO}_2\text{-50 mol % Gd}_2\text{O}_3)$ ,

$\text{CeO}_2\text{-(50 mol % La}_2\text{O}_3\text{-50 mol % Gd}_2\text{O}_3)$  and two isoconcentrates 15 and 45 mol %  $\text{CeO}_2$ .

In the  $\text{CeO}_2\text{-La}_2\text{O}_3\text{-Gd}_2\text{O}_3$  system at 1500 °C and 1250 °C new phases were not detected. At the investigated temperatures, fields of solid solutions based on cubic (F) with a fluorite-type structure of  $\text{CeO}_2$  modifications, monoclinic (B) and cubic (C) modifications

of Gd<sub>2</sub>O<sub>3</sub>, and hexagonal (A) modifications of La<sub>2</sub>O<sub>3</sub> are formed in the system.

Based on the obtained results, an isothermal cross-section of the state diagram of the CeO<sub>2</sub>–La<sub>2</sub>O<sub>3</sub>–Gd<sub>2</sub>O<sub>3</sub> system at 1500 °C was constructed (Figure 7). The initial chemical and phase composition of the samples fired at 1500 °C are shown in table S4.

To determine the position of the boundaries of the phase fields, along with the data on the phase composition of the samples, we used the concentration dependences of the parameters of the unit cells of the formed phases (Figures 8–11).

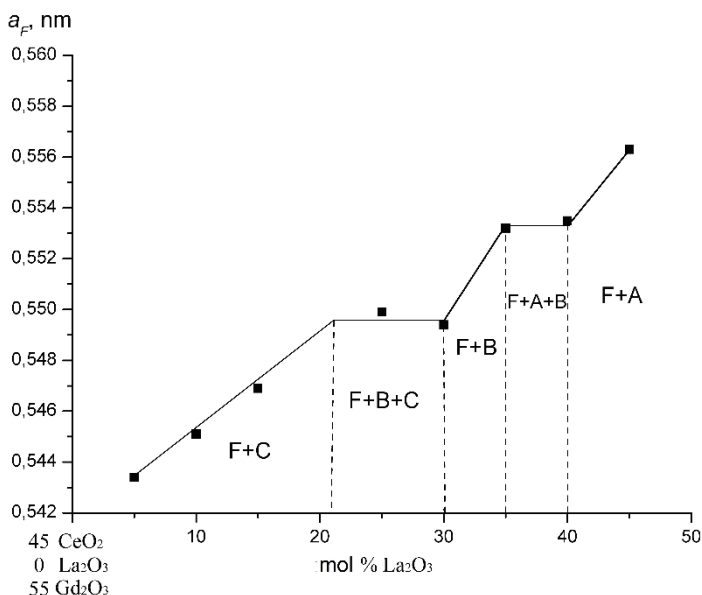


**Figure 9.** Concentration dependence of parameters of *a* elementary cells of solid solutions with fluorite-type structure (F-CeO<sub>2</sub>) of CeO<sub>2</sub>–La<sub>2</sub>O<sub>3</sub>–Gd<sub>2</sub>O<sub>3</sub> system along isoconcentrate of 45 mol % CeO<sub>2</sub> after heat treatment of samples at 1500°C

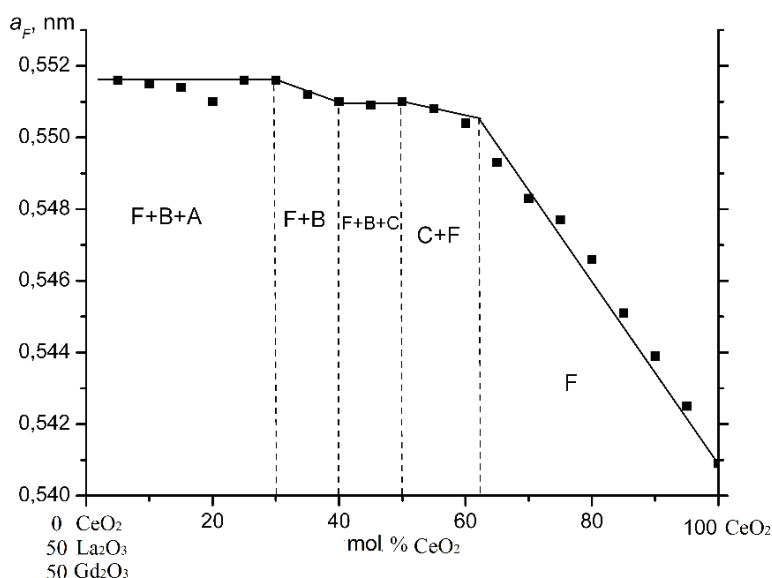


**Figure 10.** Concentration dependence of parameters of *a* elementary cells of solid solutions with structure of fluorite type (F-CeO<sub>2</sub>) of CeO<sub>2</sub>–La<sub>2</sub>O<sub>3</sub>–Gd<sub>2</sub>O<sub>3</sub> system in cross section CeO<sub>2</sub>– (50 mol% La<sub>2</sub>O<sub>3</sub>–50 mol% Gd<sub>2</sub>O<sub>3</sub>) after heat treatment of samples at 1500°C.

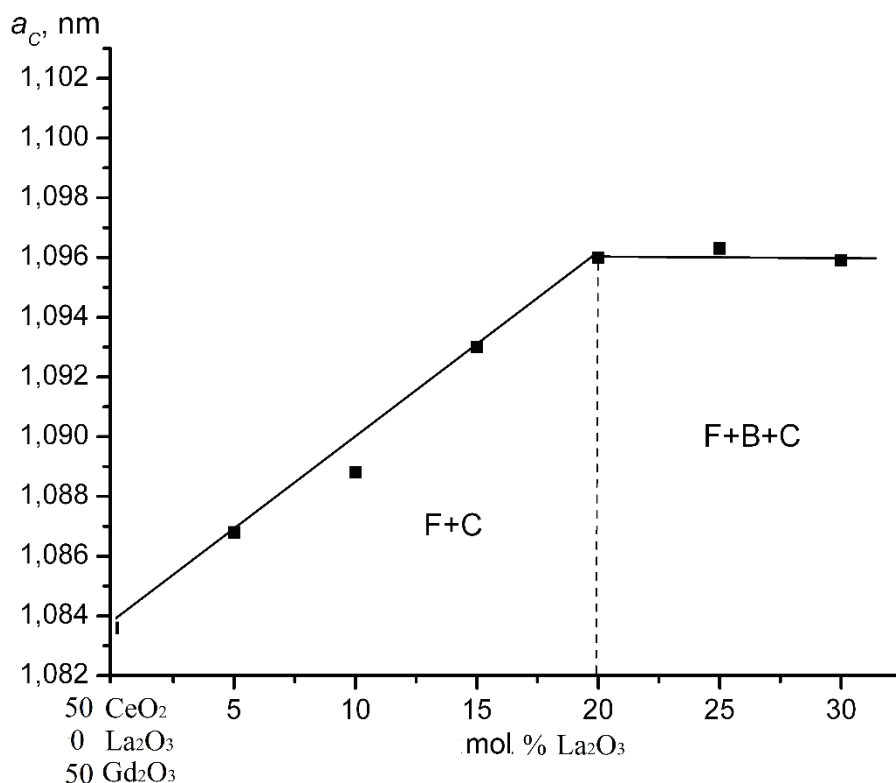


**Figure 11.** Concentration dependence of the parameters of the elementary cells of cubic solid solutions of C-Gd<sub>2</sub>O<sub>3</sub> system CeO<sub>2</sub>-La<sub>2</sub>O<sub>3</sub>-Gd<sub>2</sub>O<sub>3</sub> in the cross section La<sub>2</sub>O<sub>3</sub>-(50 mol% CeO<sub>2</sub>-50 mol% Gd<sub>2</sub>O<sub>3</sub>) after heat treatment of samples at 1500°C

The largest region of homogeneity of this isothermal cross-section is occupied by solid solutions with a structure of the fluorite type (F-CeO<sub>2</sub>). Based on the literature data [32-34] and the results obtained in this study, it was found that with a change in one of the components in a number of studied systems CeO<sub>2</sub>-La<sub>2</sub>O<sub>3</sub>-Ln<sub>2</sub>O<sub>3</sub> and, accordingly, a decrease in the ionic radius from Sm<sup>3+</sup> (0.100 nm) to Gd<sup>3+</sup> (0.0972 nm) there is a decrease in the region of homogeneity of cubic solid solutions of F-CeO<sub>2</sub>, which is associated with the structure of boundary binary systems. The boundary of the region of homogeneity of the above-mentioned solid solutions extends from the corresponding coordinates in the limiting binary systems CeO<sub>2</sub>-La<sub>2</sub>O<sub>3</sub> (100-51 mol % CeO<sub>2</sub>) and CeO<sub>2</sub>-Gd<sub>2</sub>O<sub>3</sub> (100-85 mol % CeO<sub>2</sub>).

The unit cell parameters of F-CeO<sub>2</sub> solid solutions vary from  $a = 0.5409$  nm for pure CeO<sub>2</sub> to  $a = 0.5504$  nm for a two-phase sample (F + C), containing 60 mol % CeO<sub>2</sub>-20 mol % La<sub>2</sub>O<sub>3</sub>-20 mol % Gd<sub>2</sub>O<sub>3</sub> and up to  $a = 0.5510$  nm for a three-phase sample (F + B + C), containing 50 mol % CeO<sub>2</sub>-25 mol % La<sub>2</sub>O<sub>3</sub>-25 mol % Gd<sub>2</sub>O<sub>3</sub>, as well as up to  $a = 0.5512$  nm for a two-phase sample (F + B), containing 35 mol % CeO<sub>2</sub>-32.5 mol % La<sub>2</sub>O<sub>3</sub>-32.5 mol % Gd<sub>2</sub>O<sub>3</sub> and up to  $a = 0.5512$  nm for a three-phase sample (F + B + A), containing 30 mol %

CeO<sub>2</sub>-35 mol % La<sub>2</sub>O<sub>3</sub>-35 mol % Gd<sub>2</sub>O<sub>3</sub> in the cross section of CeO<sub>2</sub> - (50 mol % La<sub>2</sub>O<sub>3</sub>-50 mol % Gd<sub>2</sub>O<sub>3</sub>), (Figure 10). Therefore, it follows from the presented results that cubic solid solutions of F-type are stored up to 62 mol % CeO<sub>2</sub>. It was found that the values of the unit cell parameters increase, because the concentration of trivalent ions embedded in the crystal lattice (La<sup>3+</sup> (0.114 nm) and Gd<sup>3+</sup> (0.0972 nm)) increases in Figure 10. Probably, the replacement of the tetravalent ion Ce<sup>4+</sup> by the trivalent ion Ln<sup>3+</sup> is accompanied by the simultaneous inclusion of vacancies of oxygen ions. Obviously, in the studied system, the relative effect of ion size dominates over the effect of oxygen vacancy. When you reach 65 mol % CeO<sub>2</sub>, the formation of an ordered C-type phase and the transition to a two-phase region (F + C) is observed. Thus, with increasing concentration of La<sup>3+</sup> and Gd<sup>3+</sup> in CeO<sub>2</sub>, more vacancies of oxygen ions are created, which are the driving force of ordering, resulting in the formation of a C-type crystal structure. In a composition containing 50 mol % CeO<sub>2</sub>, there is a saturation of Gd<sup>3+</sup> ions, resulting in the formation of a monoclinic solid solution of B-Gd<sub>2</sub>O<sub>3</sub> and the transition to the three-phase region. A similar situation is observed in the sample containing 30 mol % CeO<sub>2</sub>, in which the formation of hexagonal solid solutions of A-La<sub>2</sub>O<sub>3</sub> happens. In the concentration range of 30-2 mol % CeO<sub>2</sub> the formation

of a three-phase region (F + A + B) is observed. Along the ray  $\text{La}_2\text{O}_3$ –(50 mol %  $\text{CeO}_2$ –25 mol %  $\text{Gd}_2\text{O}_3$ ), the unit cell parameters of F– $\text{CeO}_2$  solid solutions increase from  $a = 0.5418$  nm for a two-phase sample of 50 mol %  $\text{CeO}_2$ –0 mol %  $\text{La}_2\text{O}_3$ –50 mol %  $\text{Gd}_2\text{O}_3$  to  $a = 0.5478$  nm for a three-phase sample (F + C + B), containing 40 mol %  $\text{CeO}_2$ –20 mol %  $\text{La}_2\text{O}_3$ –40 mol %  $\text{Gd}_2\text{O}_3$  and up to  $a = 0.5502$  nm for a two-phase sample (F + B), containing 32.5 mol %  $\text{CeO}_2$ –35 mol %  $\text{La}_2\text{O}_3$ –32.5 mol %  $\text{Gd}_2\text{O}_3$ , as well as up to  $a = 0.5526$  nm for a three-phase sample (F + B + A), containing 30 mol %  $\text{CeO}_2$ –40 mol %  $\text{La}_2\text{O}_3$ –30 mol %  $\text{Gd}_2\text{O}_3$  and up to  $a = 0.5546$  nm for a two-phase sample (F + A), containing 17.5 mol %  $\text{CeO}_2$ –65 mol %  $\text{La}_2\text{O}_3$ –17.5 mol %  $\text{Gd}_2\text{O}_3$ . From the presented data it follows that the tendency to increase the parameters of the unit cell persists and the substitution process is similar to the above ray. The results of X-ray phase analysis are consistent with the data of microstructural studies. It is

established that the composition of 65 mol %  $\text{CeO}_2$ –17.5 mol %  $\text{La}_2\text{O}_3$ –17.5 mol %  $\text{Gd}_2\text{O}_3$  belongs to the single-phase region and has a characteristic structure for these solid solutions (Figure 12 b). At the same time, the microstructure of the sample, composition 60 mol %  $\text{CeO}_2$ –20 mol %  $\text{La}_2\text{O}_3$ –20 mol %  $\text{Gd}_2\text{O}_3$  is characterized by the presence of two structural components that differ in contrast. The basis is a dark phase matrix belonging to F– $\text{CeO}_2$ , the light phase has been identified as C– $\text{Gd}_2\text{O}_3$ .

Along the isoconcentrate 15 mol %  $\text{CeO}_2$  there is also an increase in the parameter of the unit cell F– $\text{CeO}_2$ . It is obvious that in the case of sample formulations lying along this isoconcentrate, substitution occurs mainly between  $\text{La}^{3+}$  and  $\text{Gd}^{3+}$  ions, because the concentration of  $\text{Ce}^{4+}$  ions does not change and the relative effect of ion size dominates the formation of oxygen vacancies.

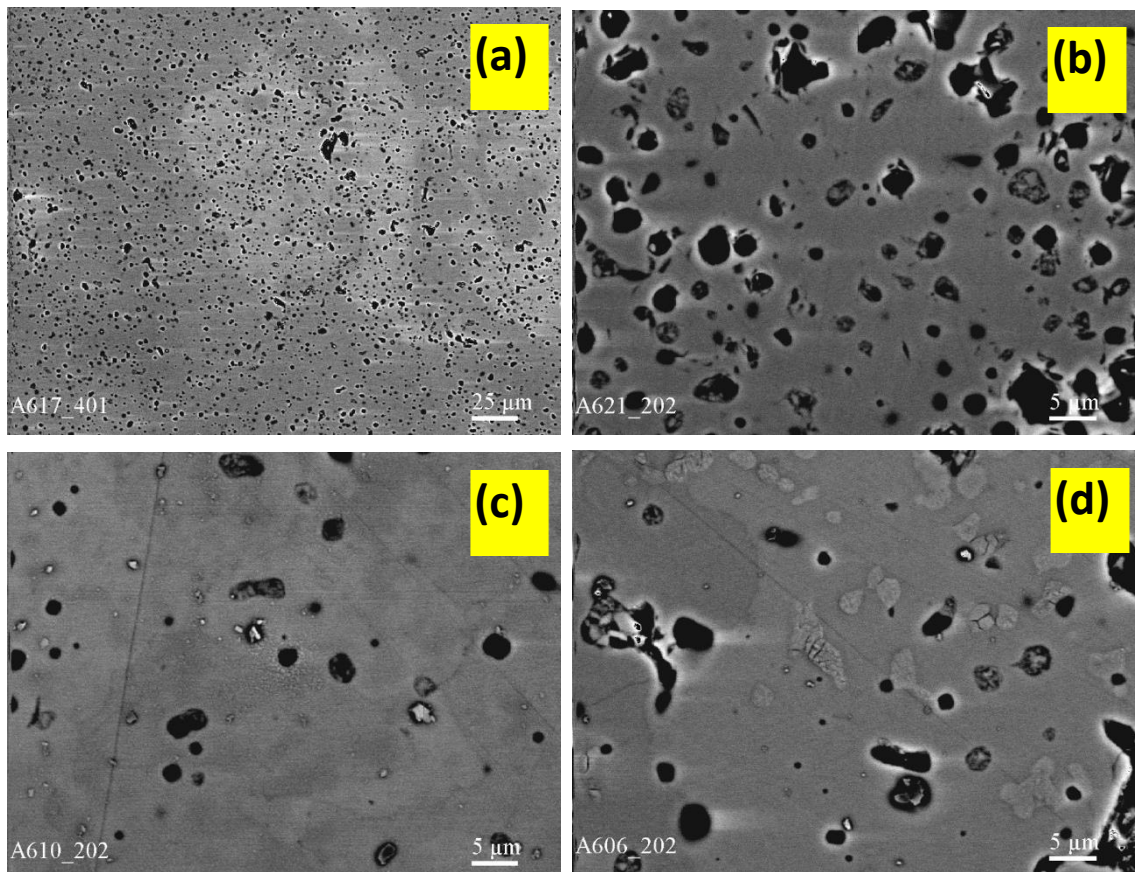


**Figure 12.** Microstructures of samples of the system  $\text{CeO}_2$ – $\text{La}_2\text{O}_3$ – $\text{Gd}_2\text{O}_3$ , after heat treatment at 1500 °C, BSE, (a) -60 mol %  $\text{CeO}_2$ –20 mol %  $\text{La}_2\text{O}_3$ –20 mol %  $\text{Gd}_2\text{O}_3$ ,  $\times 400$  (F + C); (b) -65 mol %  $\text{CeO}_2$ –17.5 mol %  $\text{La}_2\text{O}_3$ –17.5 mol %  $\text{Gd}_2\text{O}_3$ ,  $\times 400$  (F); (c) - 40 mol %  $\text{CeO}_2$ –30 mol %  $\text{La}_2\text{O}_3$ –30 mol %  $\text{Gd}_2\text{O}_3$ ,  $\times 2000$  (F + B + C); (d) - 30 mol %  $\text{CeO}_2$ –35 mol %  $\text{La}_2\text{O}_3$ –35 mol %  $\text{Gd}_2\text{O}_3$ ,  $\times 400$  (F + A + B).

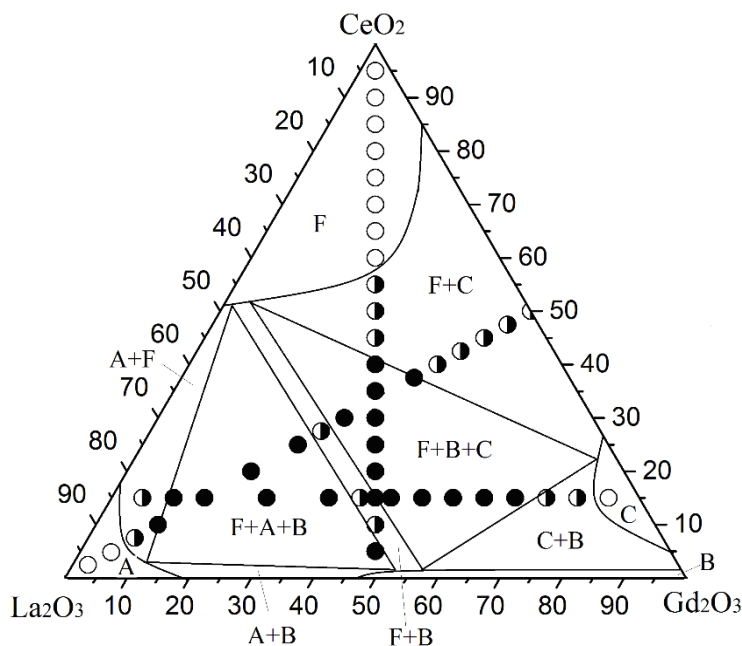


**Figure 13.** Isothermal cross section of the state diagram of the  $\text{CeO}_2\text{-La}_2\text{O}_3\text{-Gd}_2\text{O}_3$  system at 1250 °C (●- three-phase ◐ - two-phase and ○ - single-phase samples)

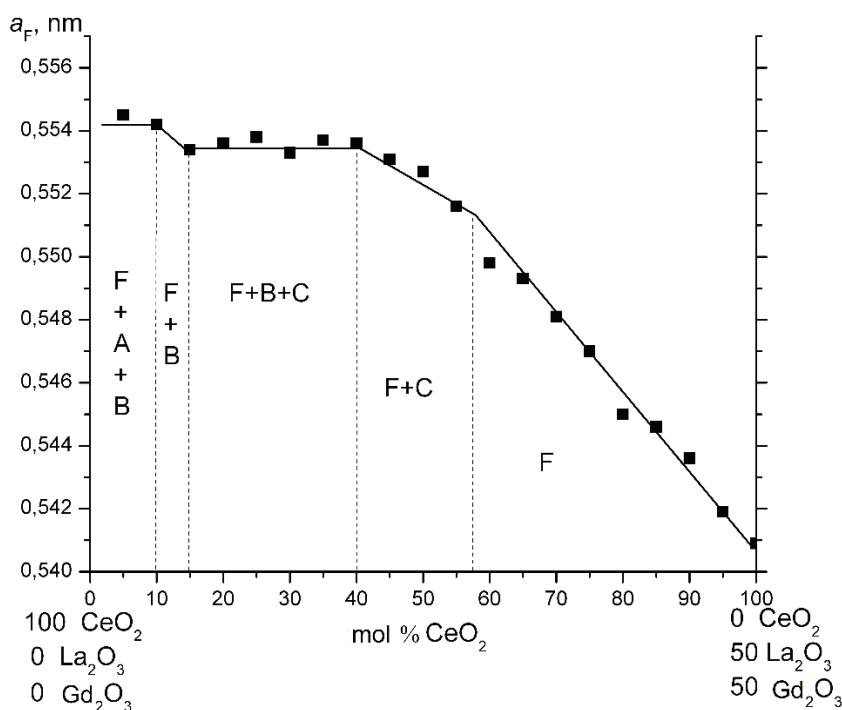


**Figure 14.** Concentration dependence of the parameters of the unit cells of cubic solid solutions based on F- $\text{CeO}_2$  on the cross section of  $\text{CeO}_2\text{-(50 mol\% La}_2\text{O}_3\text{-50 mol\% Gd}_2\text{O}_3\text{)}$  after heat treatment of samples at 1250 °C

In the corner of lanthanum oxide, a small region of homogeneity is formed on the basis of the hexagonal modification of  $\text{La}_2\text{O}_3$ . The boundary of the homogeneity region of the above solid solution extends from the corresponding coordinates in the limiting binary systems  $\text{CeO}_2\text{-La}_2\text{O}_3$  (100–25 mol %  $\text{CeO}_2$ ) and  $\text{La}_2\text{O}_3\text{-Gd}_2\text{O}_3$

(100–40 mol %  $\text{La}_2\text{O}_3$ ). From the presented data it follows that there is a decrease in the volume of the crystal lattice of solid solutions of A- $\text{La}_2\text{O}_3$ . In this case, there is an isoivalent substitution of  $\text{La}^{3+}$  by  $\text{Gd}^{3+}$  and the effective concentration of oxygen vacancies is maintained. At the same time, aliovalent substitution of  $\text{Ce}^{4+}$  by  $\text{La}^{3+}$  leads to

the filling of these vacancies with oxygen ions. Thus, it is obvious that the inclusion of vacancies and the replacement of trivalent cations, smaller in size, helps to reduce the size of the crystal lattice.

The microstructure of the sample composition is 30 mol % CeO<sub>2</sub>–35 mol % La<sub>2</sub>O<sub>3</sub>–35 mol % Gd<sub>2</sub>O<sub>3</sub> is characterized by the presence of three structural components that differ in contrast and morphology. The matrix consists of solid solutions based on F-CeO<sub>2</sub> with light inclusions, evenly distributed on the surface and identified as B-Gd<sub>2</sub>O<sub>3</sub>, the dark phase belongs to A-La<sub>2</sub>O<sub>3</sub>.

In the region with a high content of gadolinium oxide, solid solutions are formed on the basis of cubic and monoclinic modifications of lanthanide oxides. These solid solutions have small areas of homogeneity and are in equilibrium with all the phases formed in this system.

It is established that the parameters of the C-type unit cell increase with increasing concentration of La<sup>3+</sup> ions. It is certain that in the case of the formation of solid solutions based on C-Gd<sub>2</sub>O<sub>3</sub>, the relative effect of ionic size dominates over the effect of the formation of oxygen vacancies.

The isothermal cross section of the state diagram of the CeO<sub>2</sub>–La<sub>2</sub>O<sub>3</sub>–Gd<sub>2</sub>O<sub>3</sub> system has a similar structure to the previously considered systems of this series. The vast majority of isothermal cross-sections are occupied by heterogeneous regions based on solid solutions of various polymorphic modifications of the original oxides.

### 3.3 Isothermal cross section of the state diagram of the CeO<sub>2</sub>–La<sub>2</sub>O<sub>3</sub>–Gd<sub>2</sub>O<sub>3</sub> system at 1250 °C

The isothermal cross section of the state diagram of the CeO<sub>2</sub>–La<sub>2</sub>O<sub>3</sub>–Gd<sub>2</sub>O<sub>3</sub> system at 1250 °C is presented in Figure 13. The initial chemical and phase compositions of the samples fired at 1250 °C are shown in Table S5. To determine the position of the boundaries of the phase fields together with data on the phase composition of the samples used concentration dependences of the unit cells of the formed phases (Figure 14).

At 1250 °C, four regions of solid solutions of different lengths based on F- CeO<sub>2</sub>, C- and B-Gd<sub>2</sub>O<sub>3</sub>, as well as A-La<sub>2</sub>O<sub>3</sub> were found.

The lower concentration limit of the region of homogeneity of solid solutions with a fluorite-type structure is curved in the direction of decreasing cerium dioxide content and extends from the corresponding coordinates in the limiting binary systems CeO<sub>2</sub>–La<sub>2</sub>O<sub>3</sub> (100–49 mol % CeO<sub>2</sub>) and CeO<sub>2</sub>–Gd<sub>2</sub>O<sub>3</sub> (100–85 mol %

CeO<sub>2</sub>). The length of the F-phase is determined by radiographs of samples of the following compositions: 60 mol % CeO<sub>2</sub>–20 mol % La<sub>2</sub>O<sub>3</sub>–20 mol % Gd<sub>2</sub>O<sub>3</sub> - single-phase (F), 55 mol % CeO<sub>2</sub>–22.5 mol % La<sub>2</sub>O<sub>3</sub>–22.5 mol % Gd<sub>2</sub>O<sub>3</sub> - two-phase (F + C). The decrease in the region of homogeneity of the F phase is due to the structure of the limiting system CeO<sub>2</sub>– Gd<sub>2</sub>O<sub>3</sub>.

The unit cell parameters of F-CeO<sub>2</sub> solid solutions vary from a = 0.5409 nm for pure CeO<sub>2</sub> to a = 0.5516 nm for a two-phase sample (F + C), containing 55 mol % CeO<sub>2</sub>–22.5 mol % La<sub>2</sub>O<sub>3</sub>–22.5 mol % Gd<sub>2</sub>O<sub>3</sub> and up to a = 0.5536 nm for a three-phase sample (F + B + C), containing 40 mol % CeO<sub>2</sub>–30 mol % La<sub>2</sub>O<sub>3</sub>–30 mol % Gd<sub>2</sub>O<sub>3</sub> and up to a = 0.5542 nm for a two-phase sample (F + B), containing 10 mol % CeO<sub>2</sub>–45 mol % La<sub>2</sub>O<sub>3</sub>–45 mol % Gd<sub>2</sub>O<sub>3</sub> and up to a = 0.5545 nm for a three-phase sample (F + A + B), containing 5 mol % CeO<sub>2</sub>–47.5 mol % La<sub>2</sub>O<sub>3</sub>–47.5 mol % Gd<sub>2</sub>O<sub>3</sub> along the ray of CeO<sub>2</sub>– (50 mol% La<sub>2</sub>O<sub>3</sub>–50 mol% Gd<sub>2</sub>O<sub>3</sub>), (Figure 14). At 1250 °C, cubic solid solutions with a structure of the type of fluorite based on cerium dioxide are in equilibrium with all the phases formed in this system. It should be noted that with decreasing temperature to 1250 °C there is an increase in the region of homogeneity based on cubic solid solutions of F-CeO<sub>2</sub> and heterogeneous region (C + F).

Along the side of the limiting system CeO<sub>2</sub>–Gd<sub>2</sub>O<sub>3</sub>, solid solutions are formed on the basis of cubic modification of lanthanide oxides, which extend from 95 to 74 mol % Gd<sub>2</sub>O<sub>3</sub>. The solubility of La<sub>2</sub>O<sub>3</sub> in the crystal lattice of C-Gd<sub>2</sub>O<sub>3</sub> is insignificant and is 7 mol %. With a further increase in the content of La<sub>2</sub>O<sub>3</sub>, the formation of a two-phase region (C + B) is observed, because the presence in the monoclinic structure for Gd<sub>2</sub>O<sub>3</sub> is more characteristic for the specified temperature. The direction of the region of homogeneity of the C-phase probably indicates that the substitution of Gd<sup>3+</sup> ions by La<sup>3+</sup> predominates. The parameters of the unit cells of solid solutions of C-Gd<sub>2</sub>O<sub>3</sub> (Table S5) increase due to the substitution of Gd<sup>3+</sup> ions in the crystal lattice by ions with a larger ionic radius.

The region of homogeneity of B-Gd<sub>2</sub>O<sub>3</sub> occupies the smallest isothermal cross-sectional area of the state diagram of the CeO<sub>2</sub>–La<sub>2</sub>O<sub>3</sub>–Gd<sub>2</sub>O<sub>3</sub> system at 1250 °C, and slightly increases in comparison with the previously considered systems. The boundary of the region of homogeneity of solid solutions based on monoclinic modification of gadolinium oxide extends from the corresponding coordinates in the limiting binary systems CeO<sub>2</sub>–Gd<sub>2</sub>O<sub>3</sub> (100–99 mol % Gd<sub>2</sub>O<sub>3</sub>) and La<sub>2</sub>O<sub>3</sub>–Gd<sub>2</sub>O<sub>3</sub> (100–47 mol % Gd<sub>2</sub>O<sub>3</sub>). Despite the rather narrow range of homogeneity, solid solutions based on B-Gd<sub>2</sub>O<sub>3</sub> are in

equilibrium with all phases formed at this temperature, and exist in two-phase (C + B), (B + F), (A + B) and three-phase (F + B + A), (F + B + C) areas (Table S5).

Solid solutions based on hexagonal modification of lanthanum oxide have a small length. As the ionic radius of the lanthanide decreases from  $\text{Sm}^{3+}$  to  $\text{Gd}^{3+}$ , a narrowing of this region of homogeneity from 60 to 90 mol %  $\text{La}_2\text{O}_3$  is observed. It should be noted that samples with a high content of lanthanum oxide in the air hydrate, resulting in the destruction of the samples. That is, materials based on this system with a  $\text{La}_2\text{O}_3$  content of more than 60 mol % are not promising for use in the air. At the same time for samples with  $\text{La}_2\text{O}_3$  content less than 60 mol % destruction was not observed.

Based on the obtained data and the results presented in [32-35], it is possible to determine some characteristics for the state diagrams of the  $\text{CeO}_2\text{-La}_2\text{O}_3\text{-Ln}_2\text{O}_3$  series. The largest area of isothermal cross sections of these systems is occupied by cubic solid solutions with a structure of the fluorite type. As the ionic radius of the lanthanide decreases, the region of homogeneity of solid solutions based on F- $\text{CeO}_2$  narrows from 75 to 85 mol %  $\text{CeO}_2$  along the side of the limiting systems  $\text{CeO}_2\text{-Ln}_2\text{O}_3$  ( $\text{Ln} = \text{Sm}, \text{Eu}, \text{Gd}$ ), which is due to differences in their structure. The region of homogeneity of solid solutions based on the cubic C-modification of lanthanide oxides has the largest length in the  $\text{CeO}_2\text{-La}_2\text{O}_3\text{-Sm}_2\text{O}_3$  system. As the ionic radius of the lanthanide decreases, this region shifts toward the angle of the lanthanide oxide, which is due to the temperature stability of the cubic C-modification of the lanthanide oxides. During the transition to the yttrium subgroup in the systems of this series, the formation of an ordered phase with a perovskite-type structure  $\text{LaLnO}_3$  is observed. Significant dissolution of  $\text{Ce}^{4+}$  in the crystal lattice of an ordered structure of the perovskite type is not observed [35].

#### 4. Conclusion

The phase equilibria in the  $\text{La}_2\text{O}_3\text{-Gd}_2\text{O}_3$  system were studied at 1600–1100 °C in the whole concentration range. This system is characterized by the formation of limited solid solutions based on various crystalline modifications of the original components. It was found that the solubility of  $\text{Gd}_2\text{O}_3$  in the hexagonal A-modification of  $\text{La}_2\text{O}_3$  is 16 mol % at 1100 °C, 31 mol % at 1500 °C and 39 mol % at 1600 °C. The solubility of  $\text{La}_2\text{O}_3$  in monoclinic B-modification is 31, 40 and 62 mol % at 1600 1500 and 1100 °C, respectively. The formation of new phases in the  $\text{La}_2\text{O}_3\text{-Gd}_2\text{O}_3$  system has not been established.

For the first time, phase equilibria in the ternary system  $\text{CeO}_2\text{-La}_2\text{O}_3\text{-Gd}_2\text{O}_3$  were studied and isothermal cross sections at temperatures of 1500 and 1250 °C were constructed. It is established that solid solutions with fluorite (F) type structure based on  $\text{CeO}_2$  and monoclinic (B), cubic (C), hexagonal (A) modifications of  $\text{Ln}_2\text{O}_3$  are formed in the studied system. As the temperature decreases, there is a narrowing of the regions of homogeneity formed in this system. A brief description of the structure of isothermal cross sections of the  $\text{CeO}_2\text{-La}_2\text{O}_3\text{-Ln}_2\text{O}_3$  series is given. The ceria-based fluorite solid solutions are represented by the largest homogeneity field originating from the sizes of F-fields in the two boundary binary systems  $\text{CeO}_2\text{-La}_2\text{O}_3$  and  $\text{CeO}_2\text{-Gd}_2\text{O}_3$ . At 1500 and 1250 °C, cubic solid solutions with a structure of the type of fluorite based on cerium dioxide are in equilibrium with all the phases formed in this system. The isothermal sections of the  $\text{CeO}_2\text{-La}_2\text{O}_3\text{-Gd}_2\text{O}_3$  system at 1500 and 1250 °C contains two three-phase regions (F+A+B, F+B+C) and five two-phase regions (A+F, A+B, B+F, F+C, C+B). The obtained results can be used to select optimal compositions and develop new functional materials with improved characteristics.

#### Supplementary Information

Phase composition and lattice parameters of the phases in the  $\text{La}_2\text{O}_3\text{-Gd}_2\text{O}_3$ . Annealed at 1600 °C for 10 h in air (Table S1); Annealed at 1500 °C for 225 h in air (Table S2); Annealed at 1100 °C for 9820 h in air (Table S3); Annealed at 1500 °C for 130 h (Table S4).

#### References

- [1] A. Senthil Kumar, R. Balaji, S. Jayakumar, Effect of Dopant on Improving Structural, Density and Functional Properties of Ceria Based SOFC Electrolyte, *International Journal of Nanoscience and Nanotechnology*–15 (1) (2019) 37-44. [DOI]
- [2] R. Schmitt, A. Nennung, O. Kraynis, R. Korobko, A.I. Frenkel, I. Lubomirsky, S.M. Hailef, J.L.M. Rupp, A review of defect structure and chemistry in ceria and its solid solutions, *Chemical Society Reviews*, 49 (2020) 554-592.
- [3] M. Bellardita, R. Fiorenza, L. Palmisano, S. Scirè, Photocatalytic and photothermocatalytic applications of cerium oxide-based materials, *Cerium Oxide (CeO<sub>2</sub>): Synthesis, Properties and Applications* (2020) P. 109-167. [DOI]
- [4] Tiziano Montini, Michele Melchionna, Matteo Monai, and Paolo Fornasiero, *Fundamentals*

- and Catalytic Applications of CeO<sub>2</sub>-Based Materials, *Chemical Reviews*, 116 (2016) 5987–6041. [DOI]
- [5] M. Foex, F. Sibieude, A. Rouanet, D. Hernandez, Crystal-chemical effect of splat-cooling on a 30 mol % CeO<sub>2</sub> 70 mol % La<sub>2</sub>O<sub>3</sub> mixed oxide, *Journal of Materials Science*, 10 (1975) 1255–1257. [DOI]
- [6] G. Brauer, H. Gradinger, Über heterotype Mischphasen bei Seltenerdoxyden, *Zeitschrift für anorganische und allgemeine Chemie*, 276 (1954) 209–226.
- [7] G. Bacquet, C. Bouysset, and D. Hernandez, E.S.R. of Gd<sup>3+</sup> in La<sub>2</sub>O<sub>3</sub> and its solid solutions with CeO<sub>2</sub>, *Journal de Physique Colloques*, 37 (12) (1976) 204–207. [DOI]
- [8] D.J.M. Bevan and A.W. Mann, The crystal structure of Y<sub>7</sub>O<sub>6</sub>F<sub>9</sub>, *Acta Crystallographic B*, 31 (1975) 1406–1411. [DOI]
- [9] N. Minkova and S. Aslanian, Isomorphic substitutions in the CeO<sub>2</sub>–La<sub>2</sub>O<sub>3</sub> system at 850 °C, *Crystal Research Technology*, 24 (1989) P. 351–354. [DOI]
- [10] B.J. Sung, C.W. Kil, L.C. Hee, The crystal structure of ionic conductor La<sub>x</sub>Ce<sub>1-x</sub>O<sub>2-x/2</sub>, *Journal of the European Ceramic Society*, 24 (2004) 1291–1294. [DOI]
- [11] B.C. Morris, W.R. Flavell, W.C. Mackrodt, and M.A. Morris, Lattice parameter changes in the mixed oxide system La<sub>x</sub>Ce<sub>1-x</sub>O<sub>2-x/2</sub> – a combined experimental and theoretical study, *Journal of Materials Chemistry*, 3 (10) (1993) 1007. [DOI]
- [12] F. Sibieude, G. Schiffmacher, and P. Caro, Étude au microscope électronique de structures modulées dans les régions système La<sub>2</sub>O<sub>3</sub>–CeO<sub>2</sub> riches en La<sub>2</sub>O<sub>3</sub>, *Journal of Solid State Chemistry*, 23 (3-4) (1978) 361–367. [DOI]
- [13] E.R. Andrievskaya, O.A. Kornienko, A.V. Sameljuk, A. Sayir, Phase relation studies in the CeO<sub>2</sub>–La<sub>2</sub>O<sub>3</sub> system at 1100 to 1500 °C, *Journal of the European Ceramic Society*, 31 (7) (2011) 1277–1283. [DOI]
- [14] O.A. Kornienko, Interaction and properties of phases in the CeO<sub>2</sub>-Gd<sub>2</sub>O<sub>3</sub> system at 1500 °C, *Bulletin of NTU "KhPI"* 45 (2009) 86-90.
- [15] P.A. Žgung, A.V. Ruban, N.V. Skorodumova, Phase diagram and oxygen–vacancy ordering in the CeO<sub>2</sub>–Gd<sub>2</sub>O<sub>3</sub> system: a theoretical study, *Physical Chemistry Chemical Physics*, 20 (2018) 11805-11818. [DOI]
- [16] O.A. Kornienko, Interaction and properties of phases in the CeO<sub>2</sub>-Gd<sub>2</sub>O<sub>3</sub> system at 1100 °C, *Bulletin of NTU "KhPI"* 66 (2010) 14-18.
- [17] V. Grover, A.K. Tayagi, Phase Relations, Lattice Thermal Expansion in CeO<sub>2</sub>–Gd<sub>2</sub>O<sub>3</sub> System and Stabilization of Cubic Gadolinia, *Materials Research Bulletin* 39 (6) (2004) 859-866. [DOI]
- [18] A. Kossoy, Q. Wang, R. Korobko, V. Grover, Y. Feldman, E. Wachtel, A. K. Tyagi, A. I. Frenkel, and I. Lubomirsky, Evolution of the local structure at the phase transition in CeO<sub>2</sub>-Gd<sub>2</sub>O<sub>3</sub> solid solutions, *Physical Review B*, 87(5) (2013) 054101. [DOI]
- [19] O.A. Kornienko, Interaction and properties of phases in the CeO<sub>2</sub>–Gd<sub>2</sub>O<sub>3</sub> system at 600 °C, *Bulletin of NTU "KhPI"* 51 (2012) P. 50-54.
- [20] R. Horyn, A. Sikora, E. Bukowska, Phase Relations in Gd<sub>2</sub>O<sub>3</sub>–CeO<sub>2</sub>–CuO System at 980 ±C, *Acta Physica Polonica A* 106 (2004) 727-731.
- [21] E.R. Andrievskaya, Phase Equilibria in the systems of Hafnia, Ytria with rare-earth Oxides. Scientific book Project, Kiev, Naukova Dumka, 2010, 470 p.
- [22] S.A. Toropov, State diagrams of refractory oxide systems. - L.: Nauka, 1987, pp. 822. (in Russian).
- [23] M. Zinkevich, Thermodynamics of earth sesquioxides, *Progress in Materials in Science* 52 (2007) P. 597- 647. [DOI]
- [24] Yumin Zhang Thermodynamic Thermodynamic Properties of Rare Earth Sesquioxide, Supervisor: Prof In-ho Jung McGill University, Montreal, QC, Canada, Montreal – 2016.
- [25] J.P. Coutures and M. Foex, Etude a Haute TempCrature des Systsmes Formes par le Sesquioxyde de Lanthane et les Sesquioxydes de Lanthanides . I . Diagrammes de Phases (1400 °C < T < TLiquide), *Journal of Solid State Chemistry*, 182 (17) (1976) 171-182. [DOI]
- [26] R. Hory´n, E. Bukowska, A. Sikora, Phase relations in La<sub>2</sub>O<sub>3</sub>–Gd<sub>2</sub>O<sub>3</sub>–CuO system at 950 °C, *Journal of Alloys and Compounds*, 416 (2006) 209–213. [DOI]
- [27] S.J. Schneider and R.S. Roth, Phase Equilibria in Systems Involving the Rare-Earth Oxides. Part II. Solid State Reactions in Trivalent Rare-Earth Oxide Systems, *Journal of Research of the National Bureau of Standards-A. Physics and Chemistry*, 64A (4) 1960. [DOI]
- [28] O.P. Andrievska, O.A. Kornienko, O.I. Bykov Interaction of lanthanum and gadolinium oxides

- at a temperature of 1100 °C, Modern problems of physical materials science, IPM NAS of Ukraine 26 (2017) P 23–30.
- [29] M. Stopyra, I. Saenko, I. Latovskaia, G. Savinykh, O. Fabrichnaya, Phase relations in the  $ZrO_2$ – $La_2O_3$ – $Gd_2O_3$  system: experimental studies and phase modeling, *Journal American Ceramic Society* 102 (2019) 7628–7644. [[DOI](#)]
- [30] E.R. Andrievskaya, O.A. Kornienko, A.I. Bykov, Phase equilibria in the  $ZrO_2$ – $La_2O_3$ – $Gd_2O_3$  system at 1600°C, *Powder Metallurgy and Metal Ceramics* 58 (11–12) (2020) 714–724. [[DOI](#)]
- [31] O. Kornienko, O. Bykov, A. Sameliuk, O. Andrievskaya, Isothermal section structure the  $ZrO_2$ – $La_2O_3$ – $Gd_2O_3$  system at 1500 °C, *Ukrainian Chemistry Journal* 87 (1) (2021) 23–40. [[DOI](#)]
- [32] O.R. Andrievskaya, O.A. Kornienko, O.I. Bykov, O.V. Chudinovich, L.N. Spasonova, Isothermal section for the system  $CeO_2$ – $La_2O_3$ – $Eu_2O_3$  at 1500°C, *Processing and Application of Ceramics* 15 (1) (2021) 32–39. [[DOI](#)]
- [33] O.A. Korniienko, E.R. Angrievskaya, O.I. Bykov, V.S. Urbanovich, S.V. Yushkevych, L.S. Spasonova, Interaction of cerium, lanthanum and samarium oxides at 1250 °C, *Powder Metallurgy and Metal Ceramics*, 63 (2021) 342–349.
- [34] O. Kornienko, O. Bykov, A. Sameliuk, Y. Yurchenko, Phase relation studies in the  $CeO_2$ – $La_2O_3$ – $Eu_2O_3$  System at 1250 °C, *Ukrainian Chemistry Journal* 86 (3) (2020) 35–47. [[DOI](#)]
- [35] O.A. Kornienko, A.V. Sameljuk, O.I. Bykov, V. Yurchenko Yu., A.K. Barshchevskaya, Phase Relation Studies in the  $CeO_2$ – $La_2O_3$ – $Er_2O_3$  System at 1500°C, *Journal of the European Ceramic Society*, 40 (2020) 4184–4190. [[DOI](#)]

### Funding

No funding was received for conducting this study.

### Conflict of interest

The authors have no conflicts of interest to declare that they are relevant to the content of this article.

### About the License

© The author(s) 2021. The text of this article is open access and licensed under a Creative Commons Attribution 4.0 International License